International Journal of Heat and Mass Transfer 52 (2009) 2885–2892

Contents lists available at ScienceDirect

International Journal of Heat and Mass Transfer

journal homepage: www.elsevier.com/locate/ijhmt

# Low-temperature lattice thermal conductivity in free-standing GaN thin films

M.D. Kamatagi [a], R.G. Vaidya [a], N.S. Sankeshwar [a,*], B.G. Mulimani [b]

[a] Department of Physics, Karnatak University, Dharwad 580 003, India
[b] Vice-Chancellor, Gulbarga University, Gulbarga 585 106, India

ARTICLE INFO

*Article history:*
Received 25 January 2008
Received in revised form 8 September 2008
Available online 11 February 2009

*Keywords:*
Thermal conductivity
GaN
Thin films
Confined phonons
Phonon dispersion
Phonon scatterings
Defects

ABSTRACT

Low-temperature ($2 < T < 100$ K) lattice thermal conductivity, $\kappa_p$ in a semiconducting free-standing thin film (FSTF) is studied using a modified Callaway model. The quantization of acoustic phonons in FSTFs is taken into account and explicit contributions to $\kappa_p$ from the shear, dilatational and flexural modes of the confined acoustic phonons are considered. The scattering of phonons is assumed to be by sample boundaries, impurities, dislocations and other phonons via both normal and umklapp processes. Numerical results are presented for the GaN system. The phonon confinement effect, the sample finite size effect and the relative importance of confined phonon modes are investigated. The role of dislocations in limiting $\kappa_p$ is also discussed. Results are compared with those based on bulk description of acoustic phonons; bulk phonons are found to underestimate (overestimate) $\kappa_p$ in the boundary scattering regime (at higher temperatures). The calculations demonstrate that low-temperature thermal conductivity studies can lead to a better understanding of phonon scattering in FSTFs.



## 1. Introduction

In the recent past, considerable interest has been evinced in understanding the thermal properties of semiconductor nanostructures including those of GaN, which has attracted attention as a potential material system for use in high-power, high-frequency, high-temperature applications [1]. This is motivated in part, by their use in optoelectronic devices such as laser diodes and microwave power sources, where the heat dissipation places limits on device performance. Another motivation is the continued search for efficient nanostructured thermoelectric material systems. Thermoelectric materials are ranked by a figure of merit $ZT$, which is defined as $ZT = S^2\sigma T/\kappa$, where $S$ is the Seeback coefficient, $\sigma$ the electric conductivity, $\kappa$ is the thermal conductivity and $T$ is the absolute temperature; materials with higher power factor, $S^2\sigma$, and lower $\kappa$ are, therefore, preferred [2].

One of the thermal management issues in GaN technology is the presence of structural defects in the material. In GaN growth, the use of non-native substrates, such as sapphire and SiC present not only the disadvantages of lattice and thermal mismatch between the active and substrate layers, but also the possibility of unintentional contamination from the substrate during growth; typical dislocation densities reported in GaN are $N_d \sim 10^6$–$10^{10}$ cm$^{-2}$ [3]. Since any deviation from the ideal acoustical medium of a perfect crystal is known to scatter phonons, the structural imperfections in GaN, are expected to play an important role in influencing the thermal conduction in the material, particularly at lower temperatures ($T < 100$ K) [3,4].

Thermal conduction in semiconductors is mostly by acoustic phonons. The contributions to the thermal conductivity (TC) of a system are due from the various phonon scattering mechanisms and depend substantially on the temperature that determines which phonons contribute most as well as on the phonon spectrum. At low temperatures, where there is less anharmonic scattering, phonon dispersion plays an important role in thermal transport. In bulk systems, acoustic phonons are described by a nearly linear dispersion near the Brillouin zone centre. However, when acoustically mismatched barriers are present in the material, spatial confinement of phonons occurs causing a modification and quantization of the phonon spectrum. This can lead to considerable reduction in room temperature TC [5]. The phonon spatial confinement effect is expected to be particularly strong in semiconductor nanostructures, with structure feature sizes much smaller than the phonon wavelength [5–8]. The phonon wavelength in a material (which may be estimated using $\Lambda = a\theta_D/T$, where $a$ is the lattice spacing and $\theta_D$ is the Debye temperature), can exceed the structure feature size, $W$, below a certain temperature $T_m$. For instance, in the case of wurtzite (WZ) GaN thin film of width $w = 10$ nm, $T_m$ assumes values of about 22 K and 16 K for the longitudinal and transverse phonon modes, respectively.

In recent times, creation of free-standing quantum structures, with the smallest dimensions as small as a few nanometers, has

* Corresponding author. Tel.: +91 0836 2215316; fax: +91 0836 2771275, +91 0836 2747884.
*E-mail address:* n_s_sankeshwar@hotmail.com (N.S. Sankeshwar).

0017-9310/$ - see front matter © 2008 Elsevier Ltd. All rights reserved.
doi:10.1016/j.ijheatmasstransfer.2008.10.032

been made possible by the modern microfabrication techniques [9]. These structures are either solid plates or rods connected to the semiconductor substrate by the side of the smallest cross section or supported on their ends. Such free-standing quantum nanostructures, which provide two or one-dimensional confinement of electrons and phonons, have attracted interest because of their potential applications and their importance in understanding the physics of low-dimensional systems. In this paper we examine the impact of acoustic phonon confinement in isolated films. Free-standing thin films (FSTFs), also referred to as free standing quantum well structures, typically have thicknesses of about 10 nm and in-plane sizes about $2.5 \times 0.25\ \mu m^2$ [6,8]. Owing to spatial confinement induced by the free surface boundaries the phonon dispersion in FSTFs changes; it causes flattening of the dispersion curves and thereby a decrease in the phonon group velocity which, besides other factors, determines TC of the structure [5,8]. An investigation of the low-temperature TC of semiconductor nanostructures and, in particular FSTFs, which has hitherto, not been addressed, therefore becomes imperative both from the applications point of view as well as for gaining a better understanding of the physical processes participating in the thermal conduction in these structures.

The thermal properties of FSTF structures have received very little attention [5,8,10,11]. The effect of acoustic phonon confinement on the TC of FSTFs including those of GaN systems, has been studied theoretically by Balandin and co-workers [5,8]. They have shown that phonon confinement in FSTFs leads to significant decrease in the room temperature TC. Zou, et al [10] have investigated the effect of partial phonon confinement on room temperature lattice TC of nanoscale AlN/GaN/AlN heterostructures and shown that it leads to a higher TC than in a GaN thin film. Recently, Huang et al [11] have studied the thermal conduction due to confined phonons in Si thin films ($w \sim 10$–$200$ nm) in the temperature range of 300–800 K. Results for TC due to confined phonons in semiconductor nanowires are also reported [12,13].

In the present work, we investigate the effect of acoustic phonon confinement on the low-temperature ($2 < T < 100$ K) TC of FSTF structures. We employ a modified Callaway model used successfully to explain the TC data of bulk structures [4,14–17]. Including the explicit contributions from the phonon polarization branches and considering the relevant scattering mechanisms, we illustrate the effect of phonon confinement for GaN system which, being characterized by high dislocation densities ($N_d \sim 10^8 - 10^{10}$ $cm^{-2}$), will provide not only a means of assessing relative importance of phonon scattering at the defects but also a non-destructive sensitive technique to gauge the quality of the sample. In Section 2, we give the theory of TC and confined-phonon dispersions. The results of our numerical calculations are presented and discussed in Section 3. Conclusions are given in Section 4.

## 2. Theory

The TC, $\kappa$, of a material is defined, under open circuit conditions, by the relation [16]

$$U = -\kappa \nabla T, \tag{1}$$

where $U$ is the heat current density produced by the temperature gradient $\nabla T$. In general, $\kappa$ is a tensor; for an isotropic solid it is a scalar. There are, generally, two contributions to $\kappa$, namely the electronic TC, $\kappa_e$, and the lattice or phonon TC, $\kappa_p$:

$$\kappa = \kappa_e + \kappa_p. \tag{2}$$

The lattice TC, $\kappa_p$, at not too low temperatures, forms the dominant part of the TC of a semiconductor and is determined mainly by the scattering of phonons by sample boundaries, impurities, defects, other phonons and electrons.

### 2.1. Lattice thermal conductivity

The expression for lattice TC, $\kappa_p$, can be obtained by solving the Boltzmann transport equation for phonons in the relaxation time approximation, evaluating the heat current density carried by phonons and using Eq. (1). Considering heat transport by phonons of mode $s$ explicitly, $\kappa_p$, can be expressed as [15,16]

$$\kappa_p = \sum_s \kappa_s, \tag{3}$$

where each component $\kappa_s$ can be written as

$$\kappa_s = \kappa_{1s} + \kappa_{2s}. \tag{4}$$

with,

$$\kappa_{1s} = \frac{1}{3} H T^3 \int_0^{\theta_s/T} dx \frac{f(x)\tau_s^c(x)}{v_s(x)} \tag{5}$$

and

$$\kappa_{2s} = \frac{1}{3} H T^3 \frac{\left[\int_0^{\theta_s/T} dx f(x)(\tau_s^c(x)/\tau_s^N(x))\right]^2}{\int_0^{\theta_s/T} dx f(x) v_s(x)(\tau_s^c(x)/\tau_s^N(x)\tau_s^R(x))}. \tag{6}$$

Here $f(x) = x^4 e^x/(e^x - 1)^2$, $H = k_B^4/2\pi^2\hbar^3, x = \hbar\omega_s/k_B T$ and $\theta_s = \hbar(\omega_s)_{max}/k_B, (\omega_s)_{max}$ being maximum frequency of phonons of mode $s$ and $v_s(\omega_s)$ their velocity. In Eq. (6), $\tau_s^N(x)$ denotes the relaxation time for normal ($N$) phonon processes which are non-resistive, and $\tau_s^R(x)$ is the sum of all resistive ($R$) processes including those due to Umklapp phonons of mode $s$: $(\tau_s^R)^{-1} = \sum_i (\tau_i)^{-1}$, where $\tau_i$ is the phonon relaxation time corresponding to the $i$th resistive scattering process. The combined relaxation rate $(\tau_s^c)^{-1}$ can be written as $(\tau_s^c)^{-1} = (\tau_s^N)^{-1} + (\tau_s^R)^{-1}$.

In the above expressions, it may be noted that, in most of the cases, the $R$ processes dominate so that $(\tau_s^N) \gg (\tau_s^R)$ and only $\kappa_{1s}$ is important. However, when N processes become comparable to $R$ processes as, for example, in pure defect-free samples, the $\kappa_{2s}$ term contributes significantly [15–17]. In literature, most of the studies of lattice TC neglect the contribution from $\kappa_{2s}$ [5,10,11]. In the present work, we use, in our calculations, Eqs. (3)–(6) to study the behaviour of the lattice TC of FSTFs.

### 2.2. Phonon dispersions and group velocities

The elastic continuum model provides a description of the acoustic phonons for nanostructures with a confined dimension of about a few nanometers. We consider a FSTF of thickness $w$ along the growth ($z$-) direction, normal to the $(x - y)$ plane of thin film. The phonon dispersion relations can be calculated using the elasticity equation [7]

$$\frac{\partial^2 \boldsymbol{u}}{\partial t^2} = v_T^2 \nabla^2 \boldsymbol{u} + (v_L^2 - v_T^2)\nabla(\nabla . \boldsymbol{u}) \tag{7}$$

where $\boldsymbol{u}$ is the displacement vector, and $v_L$ and $v_T$ are the velocities of longitudinal and transverse bulk acoustics phonons. With the stress-free boundary conditions in the thickness direction, the FSTF supports three different types of confined phonon polarizations [7] characterized by their distinctive symmetries, namely the shear waves, dilatational waves and the flexural waves.

The shear waves have only one non zero component of $\boldsymbol{u} = (0, u_y, 0)$, which is perpendicular to the direction of wave propagation $\boldsymbol{q} = (q_x, 0)$, and lies in the plane of the quantum well. The dispersion relations for shear waves can be expressed in the form [5,7]

$$(\omega_S)_n = v_T(q^2 + q_{T,n}^2)^{1/2} \tag{8}$$

where $q_{z,n} = \pi n/w$ is the quantized wave vector in the thickness ($z$-) direction and $n$, an integer, denotes the different branches of this polarization.

The dilatational and flexural waves have two nonzero components: $\boldsymbol{u} = (u_x,0,u_z)$, with dispersion relations given by

$$(\omega_{D,F})_n = v_L(q^2 + q_{L,n}^2)^{1/2} = v_T(q^2 + q_{T,n}^2)^{1/2}. \tag{9}$$

For dilatational waves, the parameters $q_L$ and $q_T$ are determined by Eq. (9) and the transcendental equation

$$\frac{tan(q_T w/2)}{tan(q_L w/2)} = -\frac{4q^2 q_L q_T}{(q^2 - q_T^2)^2}. \tag{10}$$

The many solutions for $q_L$ and $q_T$, for each $q$, are either real or imaginary depending on the value of $q$ and $n$.

In the case flexural waves, the set of parameters $q_L$ and $q_T$, are derived from Eq. (9) and the equation

$$\frac{tan(q_L w/2)}{tan(q_T w/2)} = -\frac{4q^2 q_L q_T}{(q^2 - q_T^2)^2}. \tag{11}$$

Fig. 1 depicts the dispersion curves of a few lower branches, for the dilatational (D), flexural (F) and shear (S) waves, calculated numerically for a GaN FSTF of thickness 6 nm with $v_L = 7963\ \mathrm{ms}^{-1}$, and $v_T = 4132\ \mathrm{ms}^{-1}$ [18]. The solid, dashed and dotted lines correspond, respectively, to D, F and S waves. It is seen that, in contrast to the bulk phonon case, there are, for each polarization, an infinitely many discrete branches for a given value of $q$. At small $q$, the S and D modes have a linear dispersion, whereas the F modes have a quadratic dispersion, and hence a higher density of states. It may be noted that the D and F modes may have localized as well as propagating character depending on the branch and the in-plane wave vector [7].

The phonon group velocity for $n$th branch of a given polarization $s$ is defined as

$$v_{s,n}(\omega_s) = \frac{d(\omega_s)_n}{dq}. \tag{12}$$

The group velocities $v_{s,n}(\omega_s)$, for each branch of S,D and F modes, determined by numerical differentiation of $\omega_s$ ($q$) is found to vary with respect to branches; the higher the branch number, the smaller the group velocity. The decrease in $v_{s,n}(\omega_s)$, say, for the sixth branch of D mode is nearly two times compared to the bulk longitudinal value, $v_L$. Further, for small values of $q$, the velocities of the lowest branches of D and F modes are close to the $v_L$, and for larger $q$ the group velocities of all the three modes tend to converge to the bulk transverse velocity, $v_T$. In literature, the contributions of the discrete and infinitely many branches of the phonon modes are taken into account by either a population-weighted average group velocity [8,10] or an algebraic averaged one [12]. In the present study, with a view to investigate the role of dislocations and boundaries in influencing the low temperature TC of WZ GaN FSTFs, the algebraic averaged velocity $v_s(\omega_s)$ is considered with the total number of phonon branches contributing being assumed to be given by the ratio $w/2c$, where $c$ is the lattice constant [10]. In Fig. 2 is shown the energy dependence of the average group velocities for the D (solid line), F (dashed) and S (dotted) modes. It is seen that the averaged group velocities of all the three modes of confined phonons, at large frequencies, are smaller than the bulk transverse velocity $v_T$.

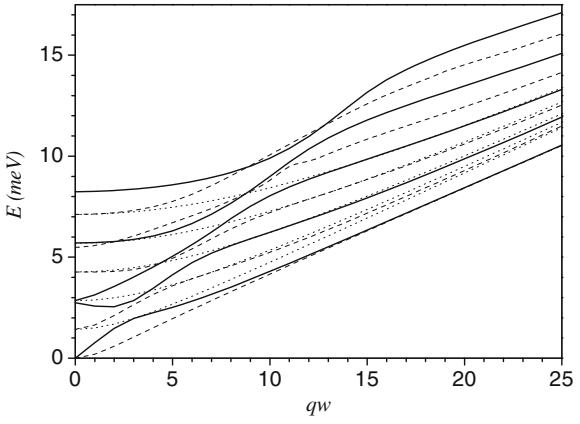


**Fig. 1.** Confined acoustic phonon dispersion for first five branches of dilatational (solid curves), flexural (dashed curves) and shear (dotted curves) modes in a GaN FSTF of width 6 nm.

### 2.3. Relaxation times

In the temperature range of interest ($2 < T < 100$ K), the resistive scattering processes limiting thermal conduction in a GaN system include the scattering of phonons by sample boundaries, various impurities and imperfections, carriers and other phonons. While the phonon–phonon scattering mechanisms are characteristic of the material, the other mechanisms are sample dependent.

#### 2.3.1. Phonon–phonon scattering

The most significant of the phonon–phonon interactions contributing to the thermal resistance in a crystal are assumed to be the normal and Umklapp three-phonon processes [19]. The three-phonon process relaxation times require a knowledge of the phonon spectrum [15,16]. However, the N processes do not contribute directly to the thermal resistance but are crucial in spreading out the influence of the other resistive processes to the entire phonon spectrum. Several forms for these relaxation times have been suggested [16,19] based on their dependences on $\omega$ and $T$.

The phonon–phonon relaxation times are taken as [15,17]:

$$(\tau_s^N)^{-1} = B_{sN}\omega_s^a T^b, \tag{13}$$

and

$$(\tau_s^U)^{-1} = B_{sU}\omega_s^2 T \exp(-C_s/T) \tag{14}$$

The scattering rate coefficients $B_{sN}$ and $B_{sU}$ typify the phonon–phonon normal and umklapp scatterings, respectively, in the material.

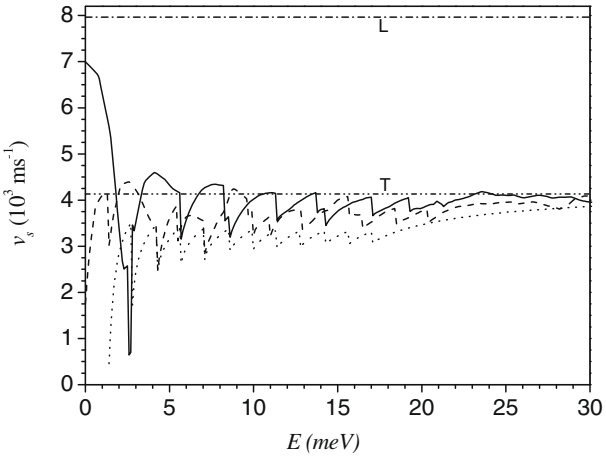


**Fig. 2.** Energy dependent average group velocity of dilatational (solid curve), flexural (dashed curve) and shear (dotted curve) phonon modes in a GaN FSTF of width 6 nm. The dash-dotted and the dash-double dotted lines represent, respectively, velocities for longitudinal and transverse bulk acoustic waves in GaN.

In literature, these quantities have been chosen to satisfy the expressions [4,15,17]

$$B_{sN} = (k_B/\hbar^2)^b[\hbar\gamma_s V_0/M[v_s(\omega_s)]^5] \quad (15)$$

$$\text{and } B_{sU} = \hbar\gamma_s^2/M[v_s(\omega_s)]^2\theta_s, \quad (16)$$

where $M$ is the average mass of an atom, $V_0$ its volume and the Gruneisen parameter $\gamma_s$ for phonons of mode $s$ is derivable from phonon dispersion relations of material system. It may be noted that the shear waves, which have the displacement vector $\boldsymbol{u}$ perpendicular to the direction of the wave propagation, are similar to bulk transverse modes in the bulk semiconductor. Similarly the D and F waves, which have a component of $\boldsymbol{u}$ in the direction of propagation, can be viewed as a modification of the bulk longitudinal mode. We accordingly, in what follows, assume that the frequency and temperature dependencies for the D and F modes and S modes are the same as those considered for longitudinal and transverse bulk phonon modes, respectively. Correspondingly, in Eq. (13) we take $(a,b) \equiv (2,3)$ for D and F modes and (1,4) for S modes[4,17]. In Eq. (8), the constant $C_s$ is assumed to scale like the Debye temperatures $\theta_s$ corresponding to phonon mode $s$; usually they are taken as $C_s = \theta_s/3$ [15,16].

*2.3.2. Sample dependent scattering*

For a typical GaN sample, the relevant sample dependent scattering mechanisms are those of phonon-boundary, phonon-defect, phonon-dislocation and phonon-disorder scatterings.

For the scattering of phonons by impurities, the relaxation time is expressed as [19]:

$$(\tau_s^I)^{-1} = \frac{V_0\Gamma}{4\pi[v_s(\omega_s)]^3}\omega_s^4 \quad (17)$$

where $\Gamma$ denotes the strength of the scattering from isotopes and point defects, such as substitutional impurities as well as possible strain in a specimen.

The scattering of phonons by boundaries, is taken as [15,19]

$$(\tau_s^B)^{-1} = [v_s(\omega_s)/L_E], \quad (18)$$

where $L_E$ represents an effective phonon mean free path of the order of the cross-sectional dimensions of the specimen. It includes effects resulting from sample size, geometry, specular reflection of phonons at the surface, etc., which may lead to deviation from the expected $T^3$ behaviour. $L_E$ can be written in the form [15]

$$L_E = \left(\frac{1}{L_C}\left(\frac{1-p}{1+p}\right) + \frac{1}{l}\right)^{-1} \quad (19)$$

for a sample of length $l$ and cross-sectional sides $b$ and $w$, the Casimir length $L_C = (4bw/\pi)^{1/2}$. The value of the specularity parameter $p$ varies from zero to one; whenever $p > 0$, partial specular reflection occurs decreasing the effect of boundary scattering.

Dislocations, inherent in GaN samples are a source of scattering of the phonons. The phonons can be scattered either by the elastic strain field surrounding the dislocation line or by the cores of the dislocation lines. The phonon scattering rate at the core of the dislocation lines is given by [19–21]

$$(\tau_s^{CD})^{-1} = \eta N_d \frac{V_0^{4/3}}{[v_s(\omega_s)]^2}\omega_s^3 \quad (20)$$

where $N_d$ is the dislocation density and $\eta$ is the weight factor to account for the mutual orientation of the direction of the temperature gradient and the dislocation line. For dislocations perpendicular to the temperature gradient $\eta = 1$, while for those parallel to the gradient $\eta = 0$; for random orientation $\eta = 0.55$.

The scattering from the strain field, for both edge and screw type dislocations, has been shown to vary as $\omega$, with a maximum scattering strength for phonons with wavevectors oriented perpendicular to the axis of the dislocation [20,21]. The phonon scattering rate by the screw and edge dislocation is given by

$$(\tau_s^{SD})^{-1} = \frac{2^{3/2}}{3^{7/2}}\eta N_d^{SD} b_s^2 \gamma_s^2 \omega_s \quad (21)$$

$$(\tau_s^{ED})^{-1} = \frac{2^{3/2}}{3^{7/2}}\eta N_d^{ED} b_E^2 \gamma_s^2 \omega_s \left[\frac{1}{2} + \left(\frac{v_L}{v_T}\right)^2\left(\frac{1-2\lambda}{1-\lambda}\right)^2\right] \quad (22)$$

where $\lambda$ is the Poisson's ratio, $b_s = c$ and $b_E = a\sqrt{2}/3$ are the magnitude of Burgers vectors for the screw and edge dislocations, respectively.

The phonon scattering rate for mixed dislocation is [20,21]

$$(\tau_s^{MD})^{-1} = \frac{2^{3/2}}{3^{7/2}}\eta N_d^{MD} \gamma_s^2 \omega_s \left[b_s^2 + b_E^2\left(\frac{1}{2} + \left(\frac{v_L}{v_T}\right)^2\left(\frac{1-2\lambda}{1-\lambda}\right)^2\right)\right] \quad (23)$$

Here $N_d^{SD}, N_d^{ED}$ and $N_d^{MD}$ are the densities of the screw, edge and mixed dislocations, respectively, and the total dislocation density is $N_d = N_d^{SD} + N_d^{ED} + N_d^{MD}$.

For the GaN samples being considered, the disorder associated with the dislocation lines can also be a source of scattering for phonons. The scattering rate is expressed as [20],

$$(\tau_s^{DO})^{-1} = \frac{c^2 a^3 N_d^2 \eta \gamma_s^2 \omega_s^2}{[v_s(\omega_s)]}, \quad (24)$$

It may be noted that, in the above equations, the spatial confinement effect enters through the confined dispersion relation. In the case of bulk description of phonons, the group velocities corresponding to those of the appropriate modes, $v_s$, assumed constant.

## 3. Results and discussion

Using the formalism described above, we present here, for the first time, an analysis of the low-temperature ($T < 100$ K) lattice TC of GaN FSTFs considering explicitly the heat conduction by shear, dilatational and flexural modes of confined acoustic phonons. In our analysis, we keep in view the typical behaviour of TC of pure semiconducting materials. Starting from temperatures above room temperature, the TC, $\kappa$, increases as $T^{-1}$ or faster with decreasing temperature, reaches a maximum $\kappa_{max}$ at $T_{max}$ around $T \sim 0.05\ \theta_D$ and falls off as $T^3$ at very low temperatures. The high-temperature behaviour is due to scattering of phonons amongst themselves whereas the $T^3$ dependence comes from that of the specific heat of the material. Near the maximum, TC is sensitive to the imperfections and impurities in the material.

Keeping in view the dominance of the various scattering mechanisms in the different temperature regions, we have performed numerical calculations of $\kappa_p\ (T)$ in the temperature range $2 < T < 100$ K for GaN FSTFs considering the dispersive nature of the confined acoustic phonons and using equations given in Section 2. With a view to bring out the effect of phonon confinement, we have also presented results for $\kappa_p$ using bulk description of phonons often used in literature [4,6,14–20]. The material parameters characteristic of WZ GaN used in the calculations are [18]: $a = 3.189$ A°, $c = 5.185$ A°, $\rho = 6100$ kg m$^{-3}$, $\lambda = 0.37$, $v_L = 7.963 \times 10^3$ ms$^{-1}$, and $v_T = 4.132 \times 10^3$ ms$^{-1}$. The Debye temperatures $\theta_s$, required in the calculations of $\kappa_p$ are taken from the respective phonon spectra. Owing to lack of experimental data on phonon spectra of FSTFs, the maximum value $(q_s)_{max}$ of the wavevector, corresponding to $(\omega_s)_{max}$, is, according to the Debye model, taken as: $q_{max} = (6\pi^2 N_A \rho/M_a)^{1/3}$, where $N_A$ is Avogadro's number and $M_a$ is atomic weight[12]. The values obtained from Fig. 1 for a FSTF of width 6 nm are $\theta_S = 361$ K, $\theta_D = 425$ K and $\theta_F = 402$ K, for shear, dilatational and flexural waves, respectively. In the case of bulk description of phonons, we assume $\theta_T = 301$ K and $\theta_L = 434$ K,

which are the values obtained from the phonon spectrum of bulk WZ GaN deduced from the second order Raman scattering experiments [4].

The important sample-dependent phonon scattering mechanisms operative in GaN, and which influence $\kappa_p$ for $T < \sim T_{max}$, are the phonon-impurity, phonon-disorder, phonon-dislocation and phonon-boundary scatterings. In our calculations we assume a typical value for the strength of the impurity scattering: $\Gamma = 10^{-4}$, a value which obtains fits for TC of bulk GaN samples [4]. With a view to investigate the roles played by the sample boundaries and the dislocations in limiting low-temperature TC we treat $L_E$ and $N_d$ as parameters; we take $\eta = 0.55$. The mode Gruniessen parameters $\gamma_s$ characterize the intrinsic phonon–phonon scattering mechanisms operative in the system. In literature a good representation of the TC of bulk GaN samples in the temperature range 4–400 K is obtained using $\gamma_L = 1.1$ and $\gamma_T = 0.45$ for the longitudinal and transverse modes, respectively [4]. Considering the S waves to be similar to the transverse waves in the bulk semiconductors and viewing the D and F waves as a modification of the bulk longitudinal mode we take, for the confined phonons, $\gamma_S = 0.45$ and $\gamma_D = \gamma_F = 1.1$.

With a view to better understand the relative importance of various sample dependent and intrinsic scattering mechanisms described, in determining the low-temperature $\kappa_p$, we first examine the variation of their relaxation rates $\tau^{-1}(\omega)$ as a function of phonon frequency, $\omega$ at $T = 77$ K. Fig. 3 depicts the frequency dependence of the various individual relaxation rates calculated for a FSTF of typical dimensions ($l \times b \times w$=) 100 μm × 100 μm × 6 nm [7–9] with $N_d = 10^{10}$ cm$^{-2}$ using Eqs. (13)–(24), but taking the overall value of $v_s$ ($\omega_s$). Curves a–d, represent the relaxation rates due to boundaries (assumed specular, $p = 1$), dislocations, impurities and other phonons, respectively. Curve 1 shows the behaviour of the overall scattering rate calculated using Matheissen's rule: $\tau^{-1}(\omega) = \sum_s (\tau_s^c(\omega_s))^{-1}$, where

$$(\tau_s^c)^{-1} = (\tau_s^B)^{-1} + (\tau_s^I)^{-1} + (\tau_s^D)^{-1} + (\tau_s^N)^{-1} + (\tau_s^U)^{-1}. \quad (25)$$

Here, the phonon–dislocation scattering rate $(\tau_s^D)^{-1}$, as depicted in the figure (curve b), includes contribution from core of dislocations, strain field of edge, screw and mixed dislocations and disorder. It is found that the dominant contribution to $\tau^{-1}(\omega)$ is from phonon–phonon scattering, for nearly the entire frequency range considered with impurity scattering becoming important for $\omega > 5 \times 10^{13}$ s$^{-1}$. Curve 2 in Fig. 3 shows the frequency dependence of $\tau^{-1}$ calculated for the diffuse boundary scattering limit ($p = 0$). It is found, in this case, that the dominant contributions to $\tau^{-1}(\omega)$ arise from sample boundaries for $\omega < 2 \times 10^{13}$ s$^{-1}$ and from other phonons for higher frequencies; the contribution from impurities and dislocations is significant for $\omega > 7 \times 10^{13}$ s$^{-1}$. For comparison, we have also evaluated the relaxation rates assuming bulk description of phonons, with a dispersion $\omega_s = v_s q$ for both longitudinal and transverse modes. Curve 3 corresponds to the overall scattering rate calculated with the bulk description of phonon modes with $p = 1.0$ and $\tau^{-1}(\omega) = \tau_L^{-1}(\omega) + 2\tau_T^{-1}(\omega)$. A comparison of curves 1 and 2 with 3 shows that the effect of phonon confinement is mostly to enhance the overall scattering rates. With a view to illustrate the phonon confinement effect for $T < T_{max}$, we choose to examine the variation of $\tau^{-1}(\omega)$ at $T = 10$ K. Its behaviour is shown in the inset of Fig. 3. Curves 1 and 3 depict, respectively, the variations of $\tau^{-1}(\omega)$ calculated (with $p = 1.0$) for confined phonons and for bulk description of the phonons. It is seen that, for $\omega < 7 \times 10^{13}$ s$^{-1}$ the confined phonon rates are lower than those calculated assuming the bulk description of phonons,. This is due to the smaller group velocity of the confined phonons, at the lower temperatures, where boundary scattering is dominant.

In the modified Callaway model employed here, heat transport by shear, dilatational and flexural phonon modes is considered explicitly. With a view to study their individual contributions to $\kappa_p$, we have performed calculations, for a FSTF of typical dimensions 100 μm × 100 μm × 6 nm [8,9], with specular boundaries ($p = 1.0$) and with $N_d = 10^{10}$ cm$^{-2}$. Curves a, b and c in Fig. 4 show the temperature variation of individual contributions to $\kappa_p$ from F, D and S phonon modes, respectively. Curve 1 represents the variation of the total TC $\kappa_p (= \kappa_S + \kappa_F + \kappa_D)$. It is seen that, for the parameters considered, $\kappa_{max}$ (~1000 W/mK) occurs at $T_{max} \sim 30$ K. Further, over a temperature range considered, the dominant contribution to $\kappa_p$ is from the S modes although both F and D modes also contribute significantly. For $T < 20$ K, where the boundary scattering is dominant, $\kappa_p$ ($\sim L_E/v_s(\omega)^2$), besides depending on the structure dimensions, is sensitive to the variation of group velocity. For $T > 20$ K, the dislocations and impurities scatter more efficiently. For $T > 50$ K, the intrinsic phonon scattering

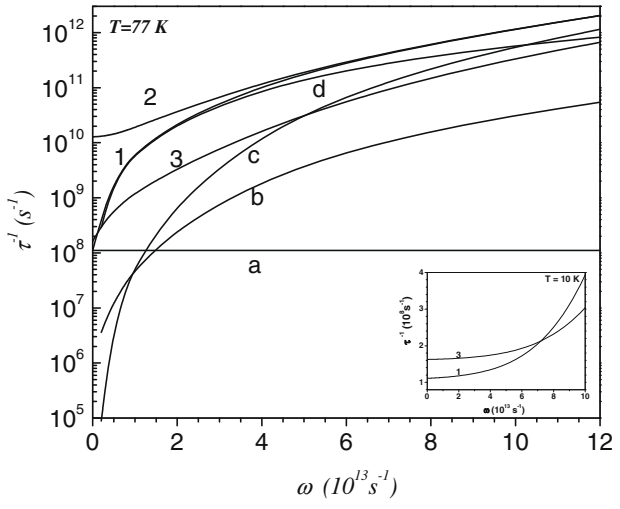


**Fig. 3.** Frequency dependence of phonon relaxation rates in a GaN FSTF of width 6 nm with $p = 1$ at $T = 77$ K, due to scattering from sample boundaries (curve a), dislocations (curve b), impurities (curve c) and other phonons (curve d). Curve 1 denotes the overall contribution. Curve 2 represents the overall contribution for $p = 0$. Curve 3 depicts the variation of overall contribution due to bulk phonons with $p = 1$. The inset shows $\tau^{-1}(\omega)$ at $T = 10$ K for confined (curve 1) and bulk (curve 3) phonons for $p = 1$.

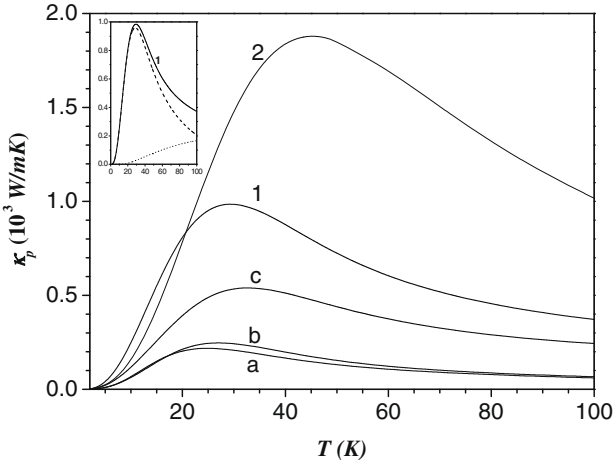


**Fig. 4.** Temperature variation of $\kappa_p$ of GaN FSTFs of width 6 nm with $p = 1$. Curves a, b and c represent the individual contributions to $\kappa_p$ from F, D and S phonon modes, respectively; curve 1 depicts the total contribution. Curve 2 shows the variation of total $\kappa_p$ due to bulk phonons. The inset shows the temperature variation of the contributions $\kappa_1$ (dashed curve) and $\kappa_2$ (dotted curve) to $\kappa_p$ (curve 1).

mechanisms become important. It may be noted that the lowest flexural mode has essentially a surface-bound character, while the lowest dilatational mode is completely localized only if the in-plane wavevector is large enough [7]. For comparison, we show the temperature variation of $\kappa_p$ calculated with bulk description of phonons in the FSTF. Curve 2 depicts the behaviour. It is found that, the degenerate transverse bulk phonon modes yield the dominant contribution to $\kappa_p$ ($=\kappa_L + 2\kappa_T$). The effect of phonon confinement, arising through the different dispersions is evident in respect of smaller magnitude and a different temperature dependence. It is seen that, for the parameters considered, the value of $\kappa_{max}$, for the confined phonons, is smaller by a factor of about two and the position of $T_{max}$ is shifted to lower temperatures. For $T > T_{max}$, where the phonon–phonon and impurity scatterings are important, the magnitude of $\kappa_p$ is found to be less than that due to the bulk phonons. Such a reduction in magnitude has been reported in the case of room temperature TC of Si FSTFs [5,11]. However, for $T < 20$ K, where the boundary scattering is effective in limiting $\kappa_p$, our calculations show that the magnitude of $\kappa_p$ calculated considering conduction with bulk description of phonons, could be underestimated. This may be attributed to larger scattering rates, in the boundary scattering regime, of bulk phonons, in comparison with those of confined phonons (see inset of Fig. 3). To estimate the contributions of $\kappa_1$ and $\kappa_2$ to $\kappa_p$, we show in the inset of Fig. 4, the temperature variation of the individual contributions $\kappa_1 (= \sum_s \kappa_{1s})$ and $\kappa_2 (= \sum_s \kappa_{2s})$ to $\kappa_p$; the dashed curve, the dotted curve and curve 1 represent $\kappa_1$, $\kappa_2$ and $\kappa_p$, respectively. It is found that, for the parameters considered, $\kappa_2$, is significant for higher temperatures. It may be noted that in literature most of the studies of lattice TC neglect the contributions from $\kappa_{2s}$ [5,10,11], a contribution originating from the momentum conserving nature of three-phonon normal processes.

With a view to understand the role of sample dependent scattering mechanisms in limiting low temperature TC in FSTFs, we first investigate the boundary-limited TC which results from the scattering of phonons at the sample surfaces. The various factors determining the effective phonon mean free path $L_E$ are the sample dimensions and the specularity parameter. In Fig. 5 is shown the temperature dependence of $\kappa_p$ calculated for a FSTF of width 6 nm with $p = 0.5$ and $N_d = 10^{10}$ cm$^{-2}$, for the samples of various in-plane dimensions ($l$ x b): 100 μm × 100 μm (Curve 1), 10 μm × 10 μm (Curve 2) and 1 μm × 1 μm (Curve 3). These dimensions corresponds to $L_E = 2.56$ μm, 0.766 μm and 0.208 μm, respectively. A comparison of curves 1,2 and 3 shows that a reduction in the in-plane dimensions of the FSTF results in a change in not only the magnitude of $\kappa_p$ but also its behaviour. The reduction in magnitude of $\kappa_p$ and the shift in the position of $T_{max}$ towards higher temperatures for smaller dimensions indicates the increasing dominance of boundary scattering. Curve 4 in Fig. 5 shows the variation of $\kappa_p$ calculated for a FSTF of width 10 nm and in-plane size 10 μm × 10 μm. A comparison of curves 2 and 4 shows that an increase in well width, increases the magnitude of $\kappa_p$, the effect of change of well-width being through $L_E$ and phonon dispersion; for the range of temperatures considered the influence of $L_E$ is found to be more (nearly 90%) than that of $v_{gs}$. To illustrate the role of the specularity parameter p in limiting TC in FSTF structures, we show in the inset of Fig. 5 the temperature dependence of $\kappa_p$ for a FSTF of dimensions 100 μm × 100 μm × 6 nm for three values of $p$. Curves a, b and c correspond to $\kappa_p$ calculated with $p = 1$, 0.5 and 0, respectively. It is seen that a decrease in the value of p from 1.0 (corresponding to $L_E = l = 100$ μm), to 0.5 (corresponding to $L_E = 2.56$ μm $\sim 3L_C$) reduces $\kappa_{max}$ by nearly four times and shifts $T_{max}$ from 29 to 66 K. When the surface scattering is diffuse ($p = 0$), $\kappa_p$ depends linearly on the sample dimensions and the effect of boundary scattering is maximum. For the sample dimensions considered, we find $L_E = 0.866$ μm, giving a value

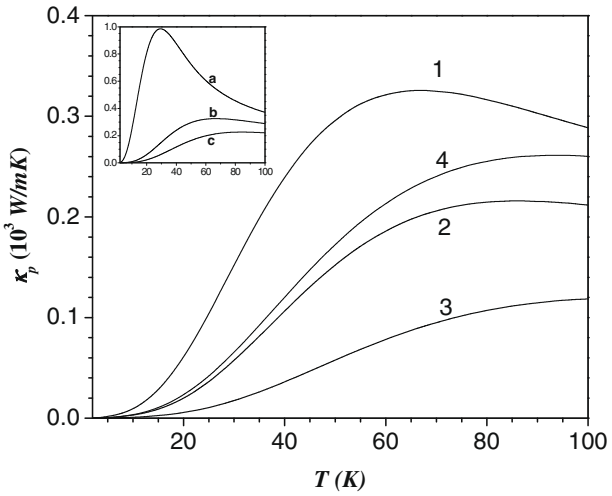


**Fig. 5.** The temperature dependence of $\kappa_p$ of GaN FSTFs of width 6 nm with $p = 0.5$ and three in-plane dimensions: 100 μm × 100 μm (curve 1), 10 μm × 10 μm (curve 2) and 1 μm × 1 μm (curve 3). Curve 4 represents variation of $\kappa_p$ of a 10 nm FSTF with in-plane dimension 10 μm × 10 μm. The inset shows the temperature variation of $\kappa_p$ of FSTF of dimensions 100 μm × 100 μm × 6 nm with $p = 1$ (curve a), $p = 0.5$ (curve b) and $p = 0$ (curve c).

$\kappa_{max} \sim 225$ W/mK at $T_{max} \sim 80$ K. It may be noted that analyses of low temperature ($0 < T < 40$ K) thermal conductance measurements, on suspended GaAs nanostructures of different geometry ($w \sim 150$ nm), have shown that diffuse surface scattering plays a major role in the phonon transport [22–24].

One of the characteristics of GaN material is that it has a large variation of dislocation densities. To illustrate the effect of dislocations on $\kappa_p$ we have studied the temperature variation of $\kappa_p$ for different dislocation densities, $N_d$. Curves 1, 2 and 3 in Fig. 6 represent $\kappa_p$ calculated for FSTF of dimensions 100 μm × 100 μm × 6 nm with $p = 1$ for $N_d = 10^8$, $10^{10}$ and $10^{12}$ cm$^{-2}$, respectively. The effect of dislocations is not only to reduce the magnitude of $\kappa_p$ but also to modify its temperature dependences. The contribution from the strain field due to screw dislocations is found to be more than that due to edge dislocations, and the contributions due to core dislocations and disorder associated with dislocations is small. Further, it

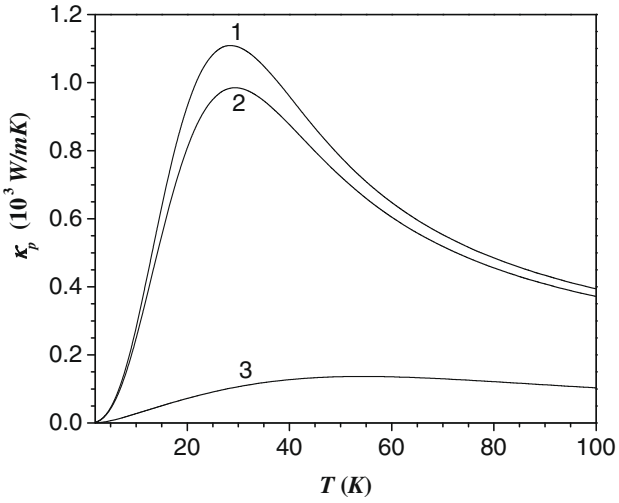


**Fig. 6.** Temperature variation of $\kappa_p$ of a GaN FSTF of dimensions 100 μm × 100 μm × 6 nm with $p = 1.0$. Curves 1,2 and 3 represent $\kappa_p$ for three values of $N_d$: $10^8$ cm$^{-2}$, $10^{10}$ cm$^{-2}$ and $10^{12}$ cm$^{-2}$, respectively.

is found that $\kappa_p$, is not sensitive to dislocations for $N_d < 10^8$ cm$^{-2}$ is as observed in bulk GaN [4,21].

To bring out the influence of phonon dispersion on the low temperature ($T < T_{max}$) TC, we have performed calculations of $\kappa_p$ for a FSTF of width 6 nm for different increasing values of $L_E$, corresponding to decreasing influence of boundary scattering. We take $p = 1.0$ and $N_d = 10^9$ cm$^{-2}$. In Fig. 7, the dotted and the dashed curves depict $\kappa_p$ calculated with $l$ ($=L_E$) = 0.6 mm and 6 mm, respectively. Curve 1 represents $\kappa_p$ for a sample assumed to be of infinite length, which corresponds to absence of boundary scattering, that is $L_E = \infty$. We find that with increase in $L_E$, the temperature dependence of $\kappa_p$ changes over from the characteristic boundary scattering $T^3$ behaviour (dotted curve) upto nearly 10 K, to a $T^2$ dependence (dashed curve) up to almost $T_{max}$, revealing the influence of dislocation scattering. With a view to assess the relative importance of the component confined phonon modes in the absence of boundary scattering, we have performed calculations of $\kappa_p$ with $L_E = \infty$. Curves a, b and c, in Fig. 7 depict, respectively, the contributions from S, D and F modes to $\kappa_p$ (curve 1). We find that, in this case for T < 10 K, the contribution from S modes is less than that from D and F modes. This may be attributed to impurity scattering becoming important (in which case $\kappa_p \sim v_s^2$) down to lower temperatures ($\sim$ 4 K), and to the smaller group velocity of S waves. It may be noted that with influence of boundary scattering being neglected, $\kappa_p$ (for $T < T_{max}$) is limited by both impurity and dislocation scatterings and for the value of $N_d$ considered, we find that the contribution to thermal resistance from dislocation scattering is only about 20%. Further, it is of interest to note that in the case of $\kappa_p$ calculated when boundary scattering and dislocations are important (that is, with $L_E = 0.1$ mm and $N_d = 10^{10}$ cm$^{-2}$) the roles of S and F modes are reversed (see Fig. 4).

It may be noted that, in the model employed here, the frequency and temperature dependencies of phonon relaxation times, often used for the bulk materials [4,15,17] may not describe correctly the phonon transport in FSTFs. Besides, in the present study, the values of the mode Gruneissen parameters $\gamma_s$ for the S, D and F modes, are taken to be constant and the same as those used for longitudinal and transverse modes of bulk phonons. An inclusion of the temperature and frequency dependences of $\gamma_s$ [17], as well as the energy and momentum conservation relations for the possible transitions between polarizations during the phonon–phonon interactions [6,25], would better describe the anharmonicity effects on the TC of FSTFs. A detailed investigation of low-temperature thermal transport in FSTFs incorporating the influence of these modifications, which could throw more light on the conduction processes, is in progress.

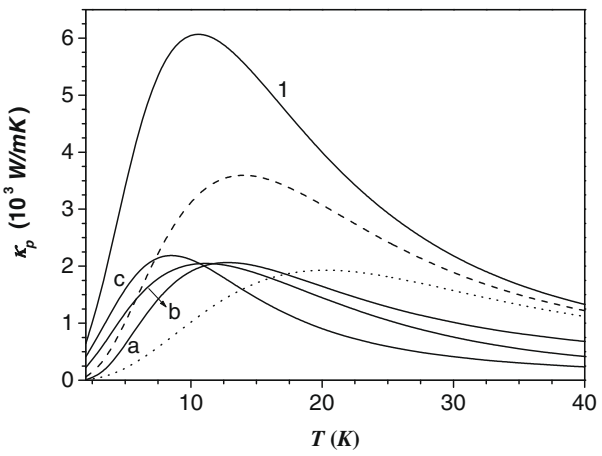


**Fig. 7.** Temperature dependence of $\kappa_p$ of a GaN FSTF of width 6 nm, with $p = 1$ and $N_d = 10^9$ cm$^{-2}$. The dotted and the dashed curves represent $\kappa_p$ calculated with $L_E = 0.6$ and 6 mm, respectively. Curves a, b and c show, respectively, the variation of individual contributions from S, D and F phonon modes, to the total TC, $\kappa_p$ (curve 1) calculated with $L_E = \infty$.

## 4. Conclusions

We have presented, for the first time, calculations of the low-temperature lattice TC for GaN free standing thin films, including the dispersive nature of the confined acoustic phonons and considering explicit contributions from shear, dilatational and flexural modes. We have employed a modified Callaway formalism, and assumed the phonons to be scattered by various sample-dependent as well as intrinsic scattering mechanisms operative in the system. We find that, for the parameters considered, the heat flow is primarily due to S mode phonons over nearly the entire temperature range considered. Further it is found that the parameters characterizing boundary scattering have an important role in determining the lattice TC. In comparison with TC calculated with bulk description of phonons, we find that although there is a significant reduction in magnitude at higher temperatures, in the boundary scattering region the magnitude due to bulk phonons may be underestimated. The relative importance of the confined phonon modes as well as the role of dislocations in limiting the TC are discussed. Detailed experimental and theoretical studies of low temperature TC of FSTFs are required to better understand the physical processes participating in the thermal conduction in these structures.

## Acknowledgement

This work is supported by UGC (India).

## References

[1] H. Morkoc, Nitride Semiconductors and Devices, Springer-Verlag, Berlin, 1999.
[2] M.L. Dresselhaus, G. Chen, M.Y. Tang, R. Yang, H. Lee, D. Wang, Z. Ren, J-P. Fleurial, P. Gogna, New directions for low-dimensional thermoelectric materials, Adv. Mater. 19 (2007) 1043–1053.
[3] A. Jezowski, B.A. Danilchenko, M. Bockowski, I. Grzegory, S. Krukoswki, T. Suski, T. Paszkiewicz, Thermal conductivity of GaN crystals in 4.2–300 K range, Solid. State Commun. 128 (2003) 69–73.
[4] M.D. Kamatagi, N.S. Sankeshwar, B.G. Mulimani, Thermal conductivity of GaN, Diamond Related Mater. 16 (2007) 98–106.
[5] A.A. Balandin, K.L. Wang, Significant decrease of the lattice thermal conductivity due to phonon confinement in a free-standing semiconductor quantum well, Phys. Rev. B 58 (1998) 1544–1549.
[6] D.G. Cahill, W.K. Ford, K.E. Goodson, G.D. Mahan, A. Majumdar, H.J. Maris, R. Merlin, S.R. Phillpot, Nanoscale thermal transport, J. Appl. Phys. 93 (2003) 793–818.
[7] N. Bannov, V. Aristov, V.V. Mitin, Electron relaxation times due to the deformation-potential interaction of electrons with confined acoustic phonons in a free-standing quantum well, Phys. Rev. B 51 (1995) 9930–9942.
[8] E.P. Pokatilov, D.L. Nika, A.A. Balandin, Phonon spectrum and group velocities in AlN/GaN/AlN and related heterostructures, Superlattices Microstruct. 33 (2003) 155–171.
[9] M.D. Williams, S.C. Shunk, M.G. Young, D.P. Docter, D.M. Tennant, B.I. Miller, Fabrication of free-standing quantum wells, Appl. Phys. Lett. 61 (1992) 1353–1354.
[10] J. Zou, X. Lange, C. Richardson, Lattice thermal conductivity of nanoscale AlN/GaN/AlN heterostructures: effects of partial phonon spatial confinement, J. Appl. Phys. 100 (2006) 104309.
[11] M.-J. Huang, T.-M. Chang, W.-Y. Chong, C.-K. Liu, C.-K. Yu, A new lattice thermal conductivity model of a thin-film semiconductor, Int. J. Heat Mass Transfer 50 (2007) 67–74.
[12] M.-J. Huang, W.-Y. Chong, T.-M. Chang, The lattice thermal conductivity of a semiconductor nanowire, J. Appl. Phys. 99 (2006) 114318.
[13] X. Lu, J.H. Chu, W.Z. Shen, Modification of lattice thermal conductivity in semiconductor rectangular nanowire, J. Appl. Phys. 93 (2003) 1219–1229.
[14] J. Callaway, Model for lattice thermal conductivity at low temperatures, Phys. Rev. 113 (1959) 1046–1051.
[15] M. Asen-Plamer, K. Bartkowski, E. Gmelin, A.P. Zhernov, A.V. Inyushkin, A. Taldenkov, V.I. Ozhogin, K.M. Itoh, E.E. Haller, Thermal conductivity of

germanium crystals with different isotope composition, Phys. Rev. B 56 (1997) 9431–9446.
[16] C.M. Bhandari, D.M. Rowe, Thermal Conduction in Semiconductors, Wiley Eastern Ltd, 1988.
[17] D.T. Morelli, J.P. Heremans, G.A. Slack, Estimation of the isotope effect on the lattice thermal conductivity of group IV and group III–V semiconductors, Phys. Rev. B 66 (2002) 195304.
[18] W. Liu, A.A. Balandin, Thermal conduction in AlxGa1–xN alloys and thin films, J. Appl. Phys. 97 (2005) 073710.
[19] P.G. Klemans, Thermal conductivity and lattice vibrational modes, in: F. Seitz, D. Turnbull (Eds.), Solid State Physics, Vol. 7, Academic Press, New York, 1958, p. 1.
[20] P.G. Klemens, The scattering of low-frequency lattice waves by static imperfections, Proc. Phys. Soc. LXVIII 12 –A (1955) 1113–1128.
[21] J. Zou, D. Kotchetkov, A.A. Balandin, D. Florescu, Fred H. Pollak, Thermal conductivity of GaN films: effects of impurities and dislocations, J. Appl. Phys. 92 (2002) 2534–2539.
[22] W. Fon, K.C. Schwab, J.M. Worlock, M.L. Roukes, Phonon scattering mechanisms in suspended nanostructures from 4 to 40 K, Phys. Rev. B 66 (2002) 045302.
[23] T.S. Tighe, J.M. Worlock, M.L. Roukes, Direct thermal conductance measurements on suspended monocrystalline nanostructures, Appl. Phys. Lett. 70 (1997) 2687–2689.
[24] Saswati Barman, G.P. Srivastava, Thermal conductivity of suspended GaAs nanostructures: theoretical study, Phys. Rev. B 73 (2006) 205308.
[25] Y.-J. Hans, P.G. Klemens, Anharmonic thermal resistivity of dielectric crystals at low temperatures, Phys. Rev. B 48 (1993) 6033–6042.